North Carolina Agricultural and Technical State University

Aggie Digital Collections and Scholarship

Theses   Electronic Theses and Dissertations

2013

Synthesis Of Pcl/Keratin Composite Nanofibers For Nerve Repair Application

Angela Michelle Edwards
North Carolina Agricultural and Technical State University

Follow this and additional works at: https://digital.library.ncat.edu/theses

Recommended Citation

Synthesis of PCL/Keratin Composite Nanofibers for Nerve Repair Application

Angela Michelle Edwards

North Carolina A&T State University

A thesis submitted to the graduate faculty

in partial fulfillment of the requirements for the degree of

MASTER OF SCIENCE

Department: Chemical, Biological and Bio Engineering

Major: Bioengineering

Major Professor: Dr. Narayan Bhattarai

Greensboro, North Carolina

2013

School of Graduate Studies
North Carolina Agricultural and Technical State University
This is to certify that the Master's Thesis of

Angela Michelle Edwards

has met the thesis requirements of
North Carolina Agricultural and Technical State University

Greensboro, North Carolina
2013

Approved by:

_____   _____
Dr. Narayan Bhattarai   Dr. Matthew McCullough
Major Professor   Committee Member

                                          _____

                                          Dr. Leonard C. Uitenham
_____   Department Chair
Dr. Jenora T. Waterman
Committee Member

             _____

             Dr. Sanjiv Sarin
             Dean, The Graduate School

Biographical Sketch

Angela Michelle Edwards was born in Fairfax, Virginia on June 22, 1986. She has obtained a Bachelor of Science degree in Physics receiving the highest honor of Suma Cum Laude at North Carolina Agricultural and Technical State University in May 2008. Currently she is working in Dr. Bhattarai's lab to complete her Master's degree in Bioengineering and expecting to finish in May 2013. The focus of her graduate research is to create and explore the characteristics of keratin based polymer nanofibers for applications to peripheral nerve regeneration and other soft tissue engineering research. Angela enjoys working in educational outreach programs with grade school students and actively volunteers in activities to support the NSF Engineering Research Center for Revolutionizing Metallic Biomaterials (ERC-RMB) program.

Dedication

This thesis is dedicated to my family and all who supported my academic career. I greatly appreciate the encouragement, love, and advice along this journey to the completion of my master's degree.

Acknowledgements

Table of Contents

List of Figures

List of Tables

List of Abbreviations

DI   Deionized

EtOH   Ethanol

FTIR   Fourier Transform Infrared Spectroscopy

IF   Intracellular intermediate filament

kV   Killovolts

mL   Milliliter

PBS   Phosphate Buffer Saline

PCL   Polycaprolactone

PEO   Poly ethylene oxide

pH   Power of Hydrogen

PHB   Polyhydroxybuturate

PLCL   Poly(DL-lactic-co-ε-caprolactone)

PLGA   Poly (D,L-lactide-co-glycolic acid

PLLA   Poly(lactic acid)

PVA   Polyvinyl alcohol

rpm   Revolutions per minute

SEM   Scanning Electron Microscopy

TFE   Trifluoroethanol

XRD   X-ray diffraction

Abstract

In the past decade, a wide variety of biomaterials comprised of both synthetic and natural polymers have been used to promote restoration of injured peripheral nerves. Despite making advances, none have matched performance of autographs, a gold standard in nerve repair. Mammalian-derived, protein-based conduits have shown good tissue biocompatibility and safe degradation products, but are mechanically fragile. Synthetic materials such as Polycaprolactone (PCL) typically have advantage of suitable mechanical properties and fine degradation rate tunability, but lack cell recognition signaling. Recent studies have shown that keratin promotes nerve cell attachment, differentiation and growth, but alone, it cannot be used as nerve guide material due to its weak mechanical performances. In the present study we extracted keratin protein from human hair and developed nanofibrous membranes of PCL/ Keratin composites by using electrospinning technique. Morphological analysis of nanofibers was done by scanning electron microscopy (SEM) and physico-chemical properties were analyzed by using X-ray diffraction (XRD), mechanical tensile testing, and Fourier Transform Infrared Spectroscopy (FTIR). Mechanical properties of PCL/Keratin nanofiber membrane showed variation in tensile strength between ratios. Potential use of these nanofibers was studied by examining the integrity in buffer solutions and cellular compatibility. PCL/Keratin fibers confirmed to have non-toxic effects on 3T3 fibroblast cells. SEM imaging showed that PCL/Keratin nanofibers promoted attachment of fibroblast cells and maintained characteristic cell morphology. Thus, appropriately constructed PCL/Keratin based composite nanofibers are expected to demonstrate the favorable biological properties of keratin and the mechanical properties of PCL. These nanofibers are found potential conduit material for peripheral nerve regeneration.

CHAPTER 1

Introduction

Damage to the peripheral nerve has been a common injury for many individuals throughout their life time. Injury to the peripheral nervous system normally affects the ability of the sensory and motor functions to perform accordingly. Documented in 1995, nearly 50,000 people experienced peripheral nerve damage restorations according to National Center for Health Statistics based on Classification of Diseases (Evans, 2001). Currently, since reported last year peripheral nerve damage has affected up to 1 million people throughout the world (Daly, Yao, Zeugolis, Windebank, & Pandit, 2012). This large scale problem can occur from numerous injuries. Historically of peripheral nerve injuries were recognized and treated as early as the Civil War era, and also be a product of normal life style habits or exercise (Mukhatyar, Karumbaiah, Yeh, & Bellamkonda, 2009) Peripheral nerve repair does not occur on a cellular level. In reality, this type of repair requires the connective tissues to be formed back together to provide a strong top outer layer to join the damaged proximal and distal ends (Matsuyama, Mackay, & Midha, 2000).

For relatively minor nerve damaged gaps natural regeneration is very probable but for larger injured nerve gaps microsurgery has been executed (Jiang, Lim, Mao, & Chew, 2010). Microsurgery is beneficial to aid natural regeneration process for gap distances greater than over a few millimeters long. For nearly 30 years the advancement of microsurgery has evolved greatly to restore peripheral nerve damage. Different techniques have been developed to progress a positive quick recovery, although recovery of severed nerves frequently do not completely heal with adequate function (Johnson, Zoubos, & Soucacos, 2005). Autographs have served as the standard for peripheral nerve damage for decades but have drawbacks such as limitations of

adequate available donor sites to replace the damaged peripheral nerve sites. Researchers and physicians have considered combining biodegradable nerve conduits to replace using autographs. Creativity of choosing specific natural and synthetic materials with certain characteristics allows materials to mimic the natural environment especially by nanofibrous materials. In general desired requirements for an ideal nerve guide conduit would include qualities of biocompatibility, biodegradability, elevated porosity, mechanically strong, and cell migration capability (Cooper, Bhattarai, & Zhang, 2011). A significant concept introduced into creating biodegradable nerve conduits was the plan of blending polymer solutions to be used in electrospinning process which creates fibrous materials. Due to specific properties such as slow degradation and excellent mechanical strength, which is necessary for peripheral nerve repair conduits, the following polymers were frequently used: poly (D,L-lactide-co-glycolic acid (PLGA), polycaprolactone (PCL), and poly(lactic acid) (Cao, Liu, & Chew, 2009).

The development of clinically applicable nerve guidance conduits requires extensive testing and consideration of the precise injured area. The gap size of the repair is a critical concern that is taken into consideration to provide the best type of materials and properties.

In this research we have developed composite nanofibers of keratin and polycaprolactone (PCL) by electrospinning method. Electrospinning is the simplest way of producing polymer fibers which have a nano scale diameter. Keratin, a naturally occurring polymer, is biorenewable, biodegradable, biocompatible, and bio-functional (Nectow, Marra, & Kaplan, 2012; Sierpinski et al., 2008). Recent studies have shown that keratin based hydrogel promotes nerve cell attachment, differentiation and growth, but alone, it cannot be used as nerve guide material due to its weak mechanical performances. PCL is a synthetic biodegradable polymer that is mechanically stronger. However, PCL generally has poor cell affinity. Thus a PCL/Keratin based

composite, is expected to demonstrate the favorable biological properties of keratin and the

mechanical properties of PCL.

CHAPTER 2

Background

2.1 Peripheral Nerve Physiology and Damage

Recurrent peripheral nerve damage continues to affect up to 1 million people worldwide per year (Daly, Yao, Zeugolis, Windebank, & Pandit, 2012). The peripheral nerves most often lose a significant amount of sensory and motor functional use after damage occurs. The intricate physiology of the peripheral nerve displayed in Figure 1 shows the layers of fibers that are in oposition to be damaged which affects sensory and motor skills function (Filler, 2004). The layers consists of the epineurium as an outer cover which is made out of conjoining tissue and blood vessels. Damage towards the outermost epineurium layer may cause significant disturbance to the flow of blood and exposed the lower layers to opposition (Tupper, 1991). Peripheral nerve fibers contain myelinated or unmyelinated fibers that vary in diameter sizes. Myelinated diameter fibers are measured 2–25 μm while unmylinated diameters range from 0.2-3.0 μm (E, 1989; Sunderland, 1951). Fascicles are formed from the collection of many nerve fibers packing together within the fibers and surrounded by perineurium. The layer of perineurium indicates the area where surgeons would suture the damaged ends together of the peripheral nerve. Figure 2 shows a visual of nerve endings being sutured together with a hollow conduit to close the gap. The physiology of peripheral nerves are further organized into three different categories. Monofascicular, oligofascicular, and polyfascicular nerves are the variety of nerves that exist. Monofascicular nerves are packed with smaller nerve fibers that contribute to motor function or sensory tasks. Oligofascicular nerves consists of fewer tiny fibers and polyfascicular nerves that are responsible to perform numerous roles (Matsuyama et al., 2000).

Damage towards any layer or category of pheriperal nervous system can result in large scale problems that are challenging to overcome.
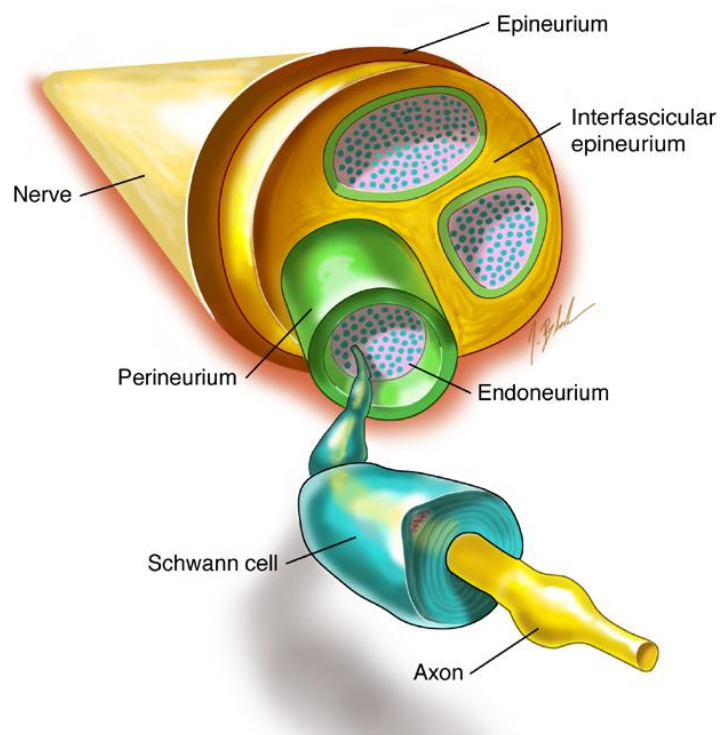
Figure 1. Schematic showing cross-sectional view of peripheral nerve.

The extent of peripheral nerve damage can be listed in three categories of neurapraxia, axonotmesis, and neurotmesis (Sunderland, 1951). Neurapraxia is the least severe type of damage where the construction of the peripheral nerve remains in position, yet disturbance of the electrical conduction occurs along the axon. A compression injury would fall in the neurapraxia category and on average lasts for hours to several weeks. Damage categorized as axonotmesis is reported when the axon is injured but the myelin sheath remains connected, which is commonly caused by a crush form of injury. Neurotmesis is the most damaging sort where nerve conduction is lost and damage to the outer connective tissue is affected. The classifications of peripheral nerve damage are listed in Table *1*. Originally, peripheral nerve damage was divided into three

categories, and then further organized into more specific categories of damage.

Table 1

Peripheral Nerve Damage Classifications

Classification 1	Classification 2	Pathophysiologic Features
Neurapraxia	Type 1	Local myelin damage
Axonotmesis	Type 2	Loss of continuity of axons; endoneurium, perineurium, and epineurium intact
	Type 3	Loss of continuity of axons and endoneurium; perineurium and epineurium intact
	Type 4	Loss of continuity of axons, endoneurium and perineurium; epineurium intact
Neurotmesis	Type 5	Complete disruption of whole nerve trunk

The worst type of peripheral nerve damage occurs when the nerve is completely severed. Peripherial nerve damaged cell bodies fracture the outermost layer of the cytoskeleton and causes the cell membrane to rupture. Swelling then occurs at the distal damaged nerve end and a stub forms at the base. Degradation transpires of both the cellular membrane and cytoskeleton which exposes the Schwann cells. The Schwann cells, which are located along the axons closest end and the myelin lipids discard as a result (Stoll, Griffin, Li, & Trapp, 1989).

2.1.1 Nerve regeneration process. The regeneration process that occurs inside empty nerve guidance conduits of peripheral nerves is summarized within five major steps and shown in a modified image in Figure 2 (Daly et al., 2012). The initial step is the fluidic phase of the regenerative process where extracellular matrix molecules are present. At this stage plasma packs the conduit (Mukhatyar et al., 2009). The next step develops the matrix in which the cables are formed joining both ends of the conduit. The third step entails cellular relocation of Schwann

cells in between the matrix fibrin cables. Configuration of tissues and proliferation access are developed during the third step as well. The forth step is titled the axonal phase, where daughter axons begin to grow across either ends of cables of tissues. Step five is when the development of myelin structures of adolescent axons is transformed into full-grown fibers. Intraluminal guidance, electrospun fiber outer layer, and functionalized surface type conduits are a few types displayed. The purpose to alter these hollow conduits is to promote an environment to allow Schwann cell passage and increase of cell production. This advancement will ultimately lead to axonal growth and will aid the nerve gap to regenerate as the hollow modified conduit degrades.
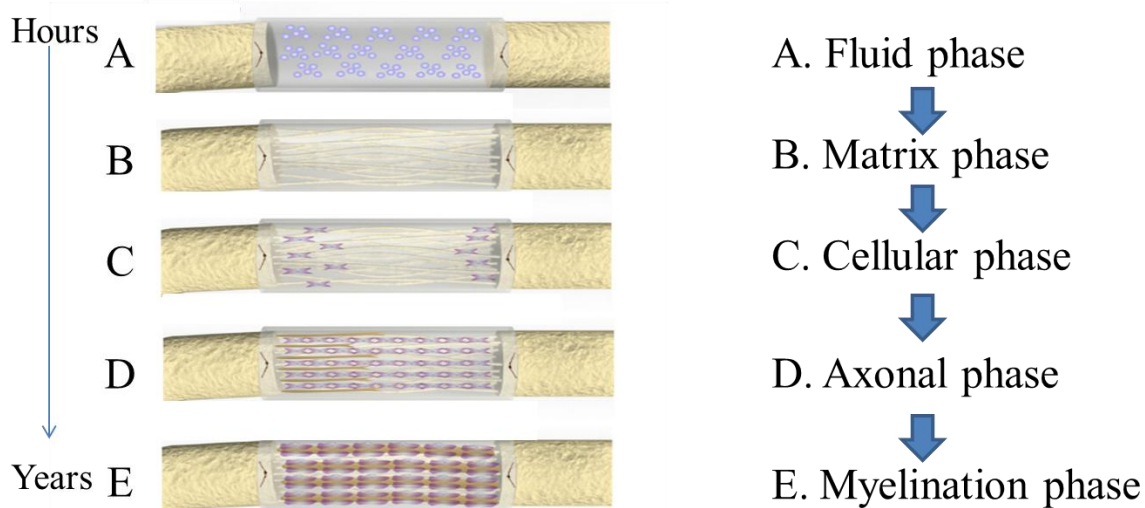
Figure 2. Process of nerve regeneration in conduits, modified from (Daly et al., 2012).

Numerous schemes have been exercised to join damaged nerve ends together. Some previous attempts included autographs, nerve guide conduits, suturing, and grafting (Mackinnon, 1989). In the past decade, a wide variety of biomaterials comprising of both synthetic and natural polymers have been utilized to promote the regeneration of injured nerves. (Nectow et al., 2012; Sierpinski et al., 2008) Despite making advances with these materials, none have matched performance of autographs, a gold standard in nerve repair. Autographs shares the biological similarity and structure that closely relates to the damaged peripheral nerve (Jiang et

al., 2010).   In many cases, autographs have limitations at both the donor and nerve gap sight which ultimately results in greater chance of losing function. This major drawback of inadequate function also often causes additional grafting to form at the donor site (Prabhakaran, Venugopal, Chyan, et al., 2008). Purposely the vein autograph has been utilized for nerve gap damages of length up to 3 cm long and has reported varying results in diverse studies. Results from a particular study reported 85% success rate in cases for nerve defects ranging from 0.5 to 6cm in length (Battiston, Tos, Geuna, Giacobini-Robecchi, & Guglielmone, 2000). Another study reported an increase of thickness in axon diameter and myelin sheath using inside-out repair techniques compared to standard vein grafting (Kelleher et al., 2001). Autographs also promote the need for supplementary surgeries which increases the chance for infection and prolongs overall healing time. Additionally to these complications development of neuromas can occur as a result to surgery (Nectow et al., 2012).

In 1876 nerve grafting was first introduced and explained by Albert (BN., 2011). In some cases there is possibility that donor grafts may not be as readily available as needed (Cao et al., 2009). Based on the reasons above, biomaterials have been investigated to serve as a better alternative to successfully promote regeneration of the damaged distal and proximal nerve ends.

2.2 Biomaterials Approach to Peripheral Nerve Regeneration

Previously biomaterials used for nerve guidance conduits in research included double walled poly(lactic-co-glycolic acid)/ poly(lactide) microspheres embedded within the wall of PCL nerve guides and used to repair nerve gaps of >1cm. A similar study posed to use nerve guides which incorporated glial cell lines to mend a 1.5cm nerve gap in a rat (Kokai, Bourbeau, Weber, McAtee, & Marra, 2011).   Another study incorporated laminin coating on PLGA conduits and was able to successfully gap a nerve damage area with a 15mm length (Koh et al.,

2010). Results showed better outcomes to autographs and the laminin coating encouraged guidance of cell adhesion and spreading from opposite damaged nerve ends (Itoh et al., 2003; Rutkowski, Miller, Jeftinija, & Mallapragada, 2004). Various examples previously used biomaterials and the fabrication techniques are shown in Table *2*. Some biomaterials were fabricated by blending the polymers together or having layers of materials.

Table 2

List of Commonly Used Biomaterials for Conduit Design

Material	Fabrication Technique
PLGA	Foamed and microbraided
PLLA	Gas foaming/salt leaching
Chitosan	Chitosan with aligned PGA filaments
Polyurethane/Collagen	Deposition Manufacturing
PCL/ PLGA/PLA	Rapid prototyping

2.3 Clinically Approved Nerve Guidance Conduits

Some of the listed clinically approved peripheral nerve guidance conduits are shown in Table *3*. These products were originated in the following areas around the world: Plainsboru, NJ, Birmingham, AL, The Netherlands, and Franklin Lakes, NJ. Each serves for a specific damaged gap length and degradation time. Amongst the listed materials of collagen type I, woven polyglycolic acid (PGA), poly(DL-lactic-co-ε-caprolactone)(PLCL), also other materials such as

polyvinyl alcohol (PVA) hydrogel and polyhydroxybuturate (PHB) are used to create nerve guides (Daly et al., 2012) (Nectow et al., 2012).

Table 3

Clinically Approved Nerve Guidance Conduits (Daly et al., 2012)

Product	Company	Material	Degradation Time	Max Length Gap
NeuraGen	Integra Neurosciences	Collagen type I	4 years	3cm
Neurotube	Synovis Micro Companies	Woven PGA	6-12 months	3cm
Neurolac	Polyganics Inc.	PLCL	2-3 years	3cm
Neuromatrix/Neuroflex	Collagen Matrix Inc.	Collagen type I	4-8 months	2.5cm

These clinically approved conduits have yielded data and shown promising results, but also have their limitations. Mainly, the maximum gap length is not able to exceed over 3 cm. For damaged nerve injury greater than 3 cm, there is no conduit currently available proven to be successful in aiding regeneration. In clinical and animal studies, Neurolac was reported to have some issues of swelling, biocompatibility, and degradation rate (Nectow et al., 2012). Thus, the development of a bioengineered nerve guide conduit, which could match the effectiveness of the autologous graft, would be beneficial to the field of peripheral nerve repair.

2.4 What is Keratin?

Keratin is a fibrous, sturdy, and flexible protein that serves as the core building block of hair, nails, and skin. Keratin can be extracted from additional sources such as bird feathers, shells, beaks, animal hooves, and sheep wool. The extraction process occurs through oxidation or hydrolysis which causes a chemical reaction that uses various sources of heat, water, and acid. The main purpose of keratin is to guard the epithelial cells from stresses that may possibly cause the termination of cells (Coulombe & Omary, 2002).

In particularly, keratin provides shape, integrity, and strength to the hair fiber. Typically hair fiber range from approximately 120-200 microns depending on the origin. Oxidized keratins are known as keratoses which undergo conversion of disulfide bonds and linkages in sulfonic acid groups within the hair fibers. As proteins, keratin naturally gathers to create bundles and has proliferation properties. These properties are directed by nearly 30 growth dynamics and cytokines (Lyons, Pelton, & Hogan, 1990).

2.4.1 Chemical structure of keratin. In hair, keratin molecules are arranged in bundles which are held by disulfide bonds (S-S-S-), which gives strength to hair. There are five chemical elements that compile to construct keratin. These elements are Carbon, Hydrogen, Sulfur, Oxygen, and Cysteine. Of all, Cysteine is an amino acid residue that occupies a majority of space within keratin and is highly water soluble.

The remainder chemicals form additional bonds that contribute to the keratin structure. Hydrogen and Nitrogen combine to shape alkaline amino groups ($-NH_2$) and the Carbon and Hydrogen combine together to form carboxylic acid groups (-COOH). Hair keratins have a moderately high sulfur amount in the structure and are supported by a high cross linked matrix of proteins known as the keratin-associated proteins (Moll, Divo, & Langbein, 2008). This matrix

not only provides physical support to the structure but also provides cellular contact and proliferation to be initiated and growth factors to be activated (Reichl, 2009; Sierpinski et al., 2008; Tachibana, Furuta, Takeshima, Tanabe, & Yamauchi, 2002)

2.4.2 Types of keratin. The intracellular intermediate filament (IF) family is the structural group keratins belong to. Subgroups are separated in two groups, Type I and Type II. Type I is acidic and Type II is basic to natural forms which are represented by a coiled shape, from the contact of the α- helical domain (Popescu & Hocker, 2007). Keratin is found within the cytoplasmic network of the IF that range from 10-12 nm (Coulombe & Omary, 2002). The shape of the keratin structure is shown in Figure 3. Keratins can be classified as either soft or hard, according to the amount of sulfur it contains. This quantity is directly associated with the extent of cysteine residues that form the disulfide bonds.
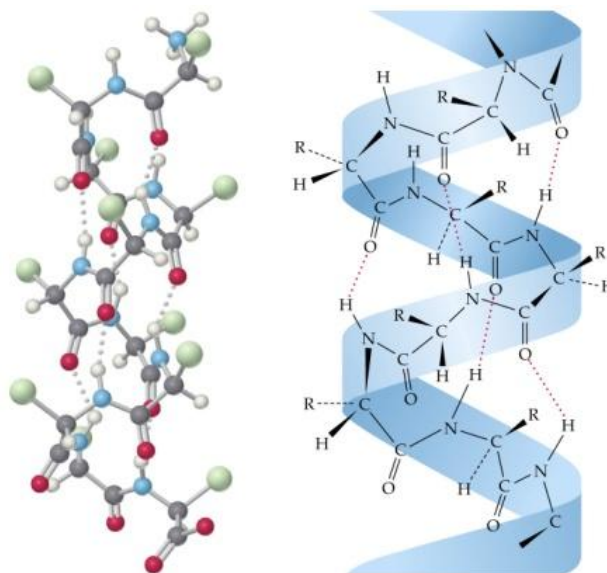

Figure 3.Basic Chemical structure of keratin.

2.4.2.1 Alpha keratins. Particularly soft keratins are determined by the low amount of sulfur that it contains. Some example structures which contain alpha keratins are hair, hoofs, horns, wool, and nails. The alpha helix provides the structure the ability to broaden and flex.

Keratins are contained and separated into three helical segments in the fibrous region of the amino acid chain. The alpha keratins which reside directly in the cortex of the hair filament has an average molecular molar mass is measured in a range of 60- 80 kDa (Hill, Brantley, & Van Dyke, 2010). This range in weight provides reduced mechanical strength properties which are necessary for nerve regenerative conduit strength. An additional contributor to strength relies on properties of beta keratins.

 2.4.2.2 Beta keratins. Hard keratins are found in tougher sources such as nails, hooves, and claws of mammals. The high amount of sulfur content makes the structure sturdy and ridged. According to Astbury, beta keratins are in the form of sheet like structures that are composed of –NH-CHR-CO$\rightarrow$ directional chains each sheet (Huggins, 1980). The adjacent chains created an antiparallel structure which launched thoughts about CO and NH group bonding in the sheets (Huggins, 1943). Beta keratins are typically harder to extract and are known not to form reconstituted configurations (Hill et al., 2010). In Table *4* comparison of various sources and the basic abilities of alpha and beta keratins are shown below.

Table 4

Alpha and Beta Keratin Comparison

	Alpha Keratins	Beta Keratins
Sources	hair, horns, sheep wool, and nails	Human fingernails, hooves, and claws of mammals, bird feathers
Ability	stretch and flex	sturdy and ridged

2.5 What is Polycaprolactone (PCL)?

 Polycaprolactone is a synthetic polymer derived from polyesters from cyclic ester lactones. Hydrolysis of PCL degrades by random chain scission of the ester groups. PCL is one of the initial synthetic polymers produce from the Carothers group in the 1930s (Carothers,

1929). PCL has the qualities of being bioresorbable, meaning PCL had the ability to be

accumulated in the body without producing toxic effects (Lam, Savalani, Teoh, & Hutmacher,

2008).

      2.5.1 Chemical structure of polycaprolactone. PCL is derived from two different

types of ring opening polymerizations of ε-caprolactone. Anionic, cationic and co-ordination or

from free radical ring opening are the alternative synthesis (Woodruff & Hutmacher, 2010).

Benefits of ring opening polymerizations include milder reaction conditions, and shorter reaction

times. The chemical structure of PCL and synthesis scheme of PCL is show in Figure 4. PCL

also has fine biodegradable and biocompatible qualities as well as the compatibility to be

blended with other polymers (Cha & Pitt, 1990). Due to breaking of the ester groups of the

polymer chains during hydrolysis, water absorption properties of PCL directly depends on the

extent of the chain length (Göpferich, 1996). PCL by itself is slow degrading polymer and has a

remarkable degradation rate > 2 years (Woodruff & Hutmacher, 2010). It has been expected that

by blending with other hydrophilic polymers, the degradation rate will be increased. Controlled

degradation is a necessary characteristic in many research investigations especially for tissue
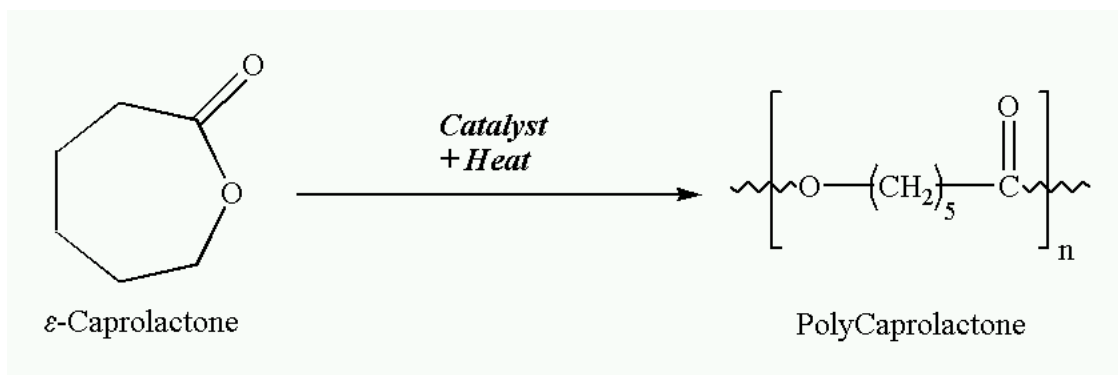
engineering scaffolds.

Figure 4. Synthesis scheme and chemical structure of PCL.

2.6 Keratin as Biodegradable Materials for Nerve Regeneration

Previous research of keratin extracted from hair has shown great potential in peripheral nerve regeneration and other tissue injury. The hair follicle possesses characteristics of cycles of growth, regression, and rest which are known as anagen, catagen, and telogen phases (Alonso & Fuchs, 2006) . These ideal characteristics can be applied to nerve regeneration purposes when keratin is extracted from hair and used as a biomaterial conduit. Keratin has also been extracted from wool and used as a biomaterial to form scaffolds. Natural polymer scaffolds should be fully biodegradable and able to be readily excreted from the body based on the healing time of the damaged nerve gap. Essentially, factors such as pore size and cell adhesion can be controlled to promote long term cell cultivation (Tachibana et al., 2002). Not only pore size can be controlled, but also controlling porosity can be achieved through a method called compression-molding/particulate-leaching to create keratin sponges extracted from wool (Katoh, Tanabe, & Yamauchi, 2004).

Interest in electrospinning keratin based nanofibers has grown over the years. Some researchers have explored blended fibers made of keratin and poly ethylene oxide (PEO). These blended fibers have the potential to be used throughout a range of areas which include protective fabrics, bioactive shells, bandages, membranes, and other biomedical devices that support improving tissue engineering (Aluigi et al., 2007). Different theories have been applied to study the interactions of keratin polymer blended solutions. The Graessley's theory was previously used to investigate the viscosity of keratin/PEO blend to further learn about the flow and change of shape of the polymer solution (Varesano, Aluigi, Vineis, & Tonin, 2008).

2.6.1 Keratin gel as filler material. Studies have shown that conduit fillers can serve as aid axonal regeneration in damaged nerve endings. A research group from Wake Forest University tested the effectiveness of keratin hydrogel fillers and developed a peripheral nerve defect model in rabbits(Paulina S. Hill & L. Andrew Koman, 2011). As a result they discovered the keratin filler to progress the conduction delay in comparison to other empty conduits. Due to the fact that the keratin filled conduits were not consistently successful, more research is required to be tested in this field. Another observation that resulted from this study was that the nerves treated with the conduit filled with keratin showed vast myelin thickness.

Keratin based hydrogel is used to advance biomedical applications such as wound healing. Naturally, wound process is composed of three phases of healing of inflammation, granulation, and remodeling. Keratinocytes, which are epidermal cells that assemble and comprise keratin, tend to travel from wound site borders to coat the entire wound site. (Clark, 1985). The presence of keratin at the wound site plays a major impact of the healing process of epithelial cell. In peripheral nerve damage keratin has been used as a conduit gel filler to provide restoration, regulate gene expression, and enhance activity of Schwann cells (Lin et al., 2012). From their study it was concluded that keratin gel filled conduits served as a more effective guide to lead Schwann cells and axon migration and to encourage proliferation of the regenerative nerve process.

2.7 PCL as Biodegradable Materials Nerve Regeneration

Polycaprolactone (PCL) is one of the most commonly used synthetic polymers used for nerve regeneration and tissue engineering applications. In studies seeking to enhance rejuvenation of tissues and peripheral nerve gaps, a polycaprolactone blend with gelatin were manufactured into nanofibrous scaffolds with different ratios. A particular ratio of 70/30

PCL/gelatin resulted as a promising blend that encourages the production of new cell production and differentiation (Ghasemi-Mobarakeh, Prabhakaran, Morshed, Nasr-Esfahani, & Ramakrishna, 2008). Researchers at the University of Pittsburgh used PC12 cells to assess the interactions with PCL and collagen based nerve guides. PCL was covered with a layer of laminin and served as an extension to cell migration and attachment across the nerve guide model (Waddell, Marra, Collins, Leung, & Doctor, 2003). PCL has contributed to the creation of numerous biomaterial based conduits blended together with adequate results of desired characteristics such as mechanical strength.

2.8 Advantages and Disadvantages of Keratin and PCL as Biomaterials

Despite the advantages of using synthetic materials, some can cause inflammatory responses. To reduce inflammatory responses, one strategy is to combine or blend synthetic materials with other more biocompatible polymers. (Nectow et al., 2012). In attempts to blend PCL with other natural polymers, it becomes opportunistic to take advantage of the ordinary biocompatibility of the natural polymer and the mechanical strength properties of PCL. The combination of the two polymers creates the needed structural stability that a nerve guide conduit should entail during the regeneration process.

2.9 Nanofibers for Peripheral Nerve Application

For peripheral nerve applications, fabrication of nanofibers is beneficial to produce nerve guide conduits. Nanofibers provide a 3-D synthetic matrix to emulate the native extra cellular matrix. They can be engineered to retain the mechanical strength and biological functionality that is needed. Nanofibers create specific geometry based on the desired parameters. Parameters required for electrospinning technology to work efficiently to produce nanofibers are dependent on numerous applications. Random fibers are created when polymer solution is electrically

charged by a high power supply source. When the electric field overcomes surface tension, of

liquid drops at the tip of electrospinning syringe, it travels toward the grounded collector and is

stretched and deposited on the aluminum foil. Spinning is controlled when the correct amount of

voltage is applied to the corresponding polymer solution. Figure 5 shows the schematic set up of

electrospinning apparatus.
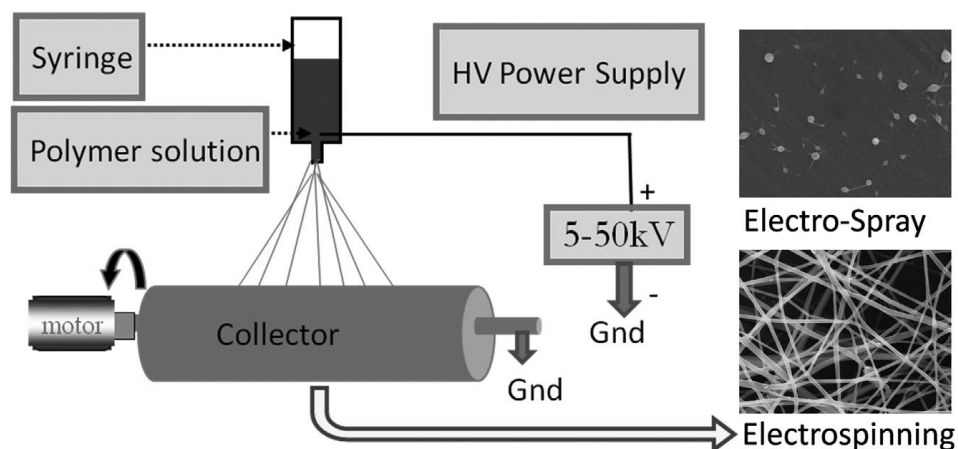
Figure 5. Electrospinning set-up.

2.10 Electrospinning Parameters (How to Control Spray vs Spinning)

The morphology of the electrospun fibers highly depends on how the polymer stream is

formed through the electrostatic environment. Electrospinning of nanofibers can only be

successful when repulsion forces surmount the surface tension of the solution. Spraying and

droplets are created on the ground collector when the repulsion force is not able to overcome the

surface tension and when additional important parameters such as solution properties and

apparatus parameters are not at optimal settings.

2.10.1 Solution properties. Polymer solutions created independently and then blended

hold key characteristics that contribute to the creation of nanofibers through electrospinning

technology. In many cases, the viscosity of the solutions is apparently a dominate parameter.

Other important characteristics of solution properties are molecular weight, surface tension, conductivity, and absorption (Beachley & Wen, 2010).

2.10.2 Apparatus parameters. Considerations included in the apparatus parameters are the high power voltage applied, the distance of the polymer solution leaving the syringe tip towards the grounded collector, the material of the collector and whether it is stationary or rotating. The surrounding conditions of the electrospinning set up such as humidity can also affect the outcomes of the nanofibers (Reneker & Chun, 1996; Reneker, Yarin, Fong, & Koombhongse, 2000).

2.11 Types of Fibers and Formation Techniques

2.11.1 Random fibers. Parameters required for electrospinning technology to successfully create random fibers are solely dependent on the grounded collector. Random fibers form when they are deposited on a stationary collector.

2.11.2 Aligned fibers. Biomedical applications in tissue engineering and peripheral nerve regeneration can require aligned fibers. Aligned nanofibers are produced by using a fast rotational grounded collector. Fibers that are traveling in the same direction can influence cellular growth and cell adhesion (Cooper et al., 2011). Aligned fibers contain extra stability and strength for the structure of the nanofibers to remain in an original shape without breaking immediately under stress. Another way to create aligned fibers is by using two split electrodes such as copper wire can be placed on the grounded collector as the fibers are being deposited (Li & Xia, 2004). The fibers collected between copper wires or other forms of electrodes can be aligned as well.

2.12 Objectives and Hypothesis

Objective 1: To develop miscible blend solution of PCL/Keratin suitable for electrospinning.

Hypothesis 1: It is hypothesized that water soluble keratin extracted from human hair will be miscible with PCL solution made in polar organic solvent e.g. Trifluoroacetic acid.

Objective 2: To develop well characterized blend nanofiber of PCL/Keratin suitable candidate for conduit for peripheral nerve gap repair.

Hypothesis 2: It is hypothesized that by mixing certain amounts of PCL with keratin, a composite nanofiber of PCL/Keratin with suitable properties such as desirable mechanical strength and cellular compatibility will be obtained.

CHAPTER 3

Methodology

3.1 Materials

3.1.1 Extraction materials. Hair was obtained from local African American barber shops in Greensboro, NC. Peracetic acid solution and Trizma ^{TM} Base powder (primary standard and buffer≥99.9% titration crystalline) was purchased from Sigma Aldrich. Hydrochloric Acid (A144C-212 Lot 093601) was purchased from Fisher Scientific.

3.1.2 Electrospinning materials. PCL, (6 caprolactone polymer, M_n70-90 kDa) and Trifluoroethanol (TFE) were obtained from Sigma Aldrich.

3.2 Extraction of Keratin

Keratin was extracted from human hair according to a previous method (Sierpinski et al., 2008) with some modifications. A summary of multiple steps involved in the extraction process is outlined in Figure 6.
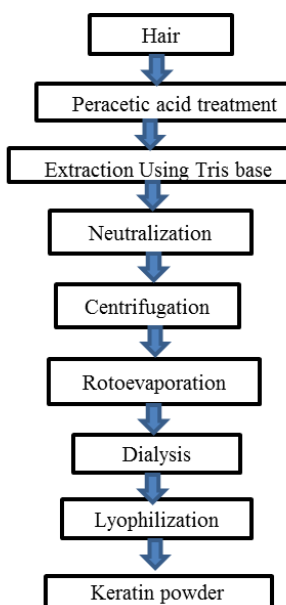

Figure 6. Keratin extraction process overview.

3.2.1 Cleaning and peracetic acid treatment. Hair was thoroughly washed with warm water and soap for a few minutes in the sink and then rinsed with DI water. Washed hair was placed in the drying oven for one hour while being frequently stirred to allow each piece of hair to dry completely. Dried hair was evenly divided into paper weigh boats and measured on an electronic balance. To save time, all stock solutions were prepared before the extraction process began and stored in the refrigerator. Peracetic Acid solution (2 wt%/vol%) was prepared under the fume hood by dissolving certain amounts of acid with water in a beaker. Peracetic acid solution was added slowly in the beaker containing hair and covered with parafilm for 12 hours.

3.2.2 Extraction of keratin in tris buffer. Hair was separated from the peracetic acid solution by using a 500 µm sieve. The hair was then thoroughly rinsed with DI water to remove residual acids and then separated evenly in two erlenmeyer flasks. The Dubnoff Metabolic Shaking Incubator was turned on and set to 38°C, 65 RPM. Stock solution of 1000mM Trizma ^{TM} Base stock solution was prepared and poured into the two flasks enough to cover the hair. Flasks were covered with parafilm and placed in the bath shaker for one hour. Liquid from each flask which contained free proteins was poured into storage and labeled as "Keratin Extract Solution". DI water was then added to both flasks, covered, and placed back in the bath shaker for another hour. Liquid was again added to the "Keratin Extract Solution".

3.2.3 Neutralization. The keratin extract solution was neutralized to approximately pH=7 using diluted hydrochloric acid solution of 30 ml of DI water and 4 ml of hydrochloric acid.

3.2.4 Centrifugation. The neutralized keratin extract solution was filled in twelve 14 ml conical tubes to be centrifuged by using VWR clinical 200 Centrifuge at 3000 rpm for 10

minutes during each cycle. Tubes were examined for collection of particles which were ultimately discarded. These steps were repeated until the entire solution was centrifuged.

3.2.5 Rotoevaporation. The Heidolph Rotary Evaporator connected with the chiller filled with DI water and ethylene glycol was assembled. The coolant chiller pump parameters were set to -25°C and cooled from 25°C to around -12°C within two hours. The rotary evaporator bath was set to 90°C and the solution was added to the rotary flask to fill it ¼ of the way full. The apparatus was lowered into the water bath until the rotary flask was submerged and the rotation speed set to 200 rpm. After 1 to 1.5 hours the rotation of the flask was stopped and apparatus was lifted to remove the flask and pour the distilled solution into storage.

3.2.6 Dialysis. Cellulose dialysis membrane (MW cut off 500 µm tubing 43mmx 27mm) was cut the desired length and secured at one end and filled with the distilled extracted solution with the aid of a funnel, and clamped secure at the top. The filled tube was placed in a 2000mL graduated cylinder and DI water was filled to cover the entire tube. The tube was left in the cylinder for 24 hours and the water was poured out and refilled ever 3-4 hours. After the 24 hour period was over, the water was emptied and the tube was taken out of the cylinder by holding the top of the tube securely and placed a beaker. The best technique discovered to empty the purified tube into the beaker successfully was to get a needle and poke holes at the bottom of the tube and allow it to drain into the beaker slowly. The mass of 80ml jars were measured, recorded, labeled alphabetically, and then filled with the solution. The jars were sealed with the cap and put in the -30⁰ overnight or until frozen.

3.2.7 Lyophilization. Lyophilization took place using the Freezone freeze dryer set to -86 °C and 0.070mBar. Samples were obtained directly from the freezer and placed into the available freeze dryer ampoules and covered with the black seals. The first ampoule was

connected to the freeze dryer by the metal rod and the knob was turned to the vacuum position.

The pressure light immediately illuminated with green lights until the pressure is below 0.133

mBar again, which indicated when another sample could be added. The samples were left on for

at least 25 hours or when completely dry.

3.3 Electrospinning of PCL/Keratin Nanofibers

      3.3.1 Polymer solution preparation. Extracted keratin was dissolved in DI water at a

concentration 10% w/v. The glass container was slowly rotated around manually or slightly tilted

and remained rested on the side to dissolve keratin on the bottom or side walls. PCL solution was

prepared by dissolving PCL granules with Trifluoroethanol (TFE) at a concentration 10% w/v.

When both the solutions were dissolved, a plastic syringe was used to remove the appropriate

amount of each solution to generate the different ratios of PCL/Keratin 100/0, 90/10, 80/20,

70/30. Each solution mixture was vortexed manually or bound by tape to secure contact for

vigorous mixing to take place. When the solution reached a blended composition, the glass vial

was immediately taken to the electrospinning apparatus in the fume hood. Figure 7 represents the

individual polymer solution preparations scheme. After mixing the solutions, the mixed blend
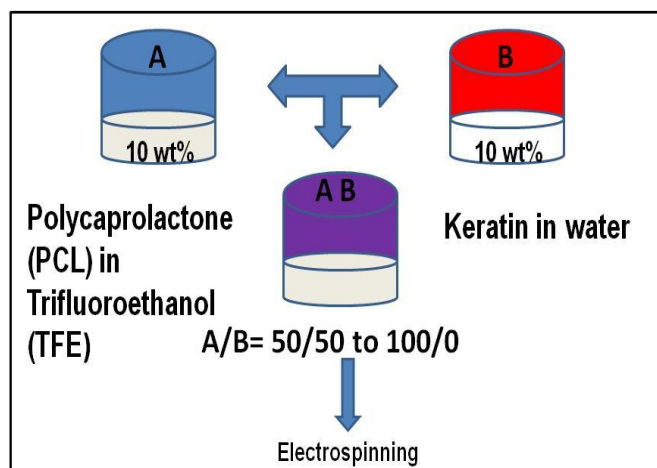
was applied for electrospinning.

Figure 7. Polymer solution preparation.

3.3.2 Electrospinning. In order to create the desired nanofibers from various polymer solutions of PCL/ Keratin 100/0, 90/10, 80/20, 85/15, 70/30, 60/40 and 50/50 specific parameters were constructed for electrospinning. The Spellman CZE100R high power voltage was safely plugged in, the aparatus was adusted correctly, and the solution was poured into the stationary syringe.   The electrically charged high power supply source was set to 25 -27 kV. When the electric field overcame surface tension, it traveled toward the stationary grounded collector and was stretched and deposited on the aluminum foil. The stationary syringe tip was approximately 16 to 23 cm away from the grounded collector and build-up at the tip of the solution while electrospinning was removed.

3.4 Characterization of Nanofibers

3.4.1 Scanning electron microscopy. Samples from each fiber ratio produced were first gold sputter coated in the Polaron SEM coating System for 1 minute and 30 seconds to guarantee even treatment. Subsequently, the samples were loaded into the SEM chamber and imaged using a 1-1.5kV accelerated voltage and 5 µA current. Additional parameters were adjusted to view a clear image in 500, 3K and 10K resolutions. All images were captured in a 40 second scanning process.

3.4.2 Fourier transform infrared spectroscopy. A FTIR spectrum was completed by using the Bruker Tensor 2 instrument. PCL/Keratin nanofibers with different ratios were tested. Samples were cut from each ratio and placed in individual conical tubes to dry under pressure for one hour. Testing was done at 200 scans and 4 cm^{-1} resolution under an absorbance mode. Figure 8 shows the different PCL/Keratin fiber samples prepared for FTIR experiment. The range of ratios prepared for testing included 100% PCL, 90/10, 80/20, 70/30, and 50/50. Testing required that fibers had a flat and solid morphology, which excluded ratio 50/50 sample to be included.

Figure 8. FTIR fiber samples.

3.4.3 X-ray diffraction. Fiber samples for XRD measurement were prepared. By cutting

each fiber membranes into a rectangular shape and contacted on a glass slide with two sided

sticky tape, length and width measurements were recorded for each fiber sample. The parameters

of the PSD detector used an absorbance =1and measured from $2\theta=10$ to 40 angle range. Scan

speed parameters were set to 1 and each scan took approximately 20 to 35 minutes to complete.

Initially the XRD was calibrated using a test sample. The sample was parallel with the rays and

the position in the z direction of the sample holder was set at a minimum -0.95 to max 1.95.
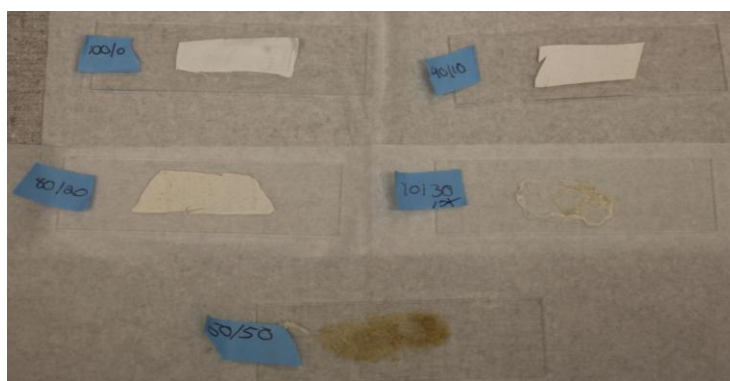

Figure 9. XRD fiber samples.

3.4.4 Mechanical strength tensile test. Each fiber sample was cut carefully and length, width and thickness for all ratios were measured. The fiber samples were measured in length and width by a regular ruler and the thickness was taken with a Digimatic micrometer for all trials. Testing was performed to collect data and three samples from each PCL/Keratin ratio were used. Fiber samples were center aligned and mounted within a 1 ¾ inch window cut from index cards and held with two sided sticky tape as shown in Figure 10. The top and bottom on the index card was measured accurately at ¾ inch length to be held by clamps on the convenient table top Shimadzu machine (North America Analytical and Measuring Instruments AGS-X series obtained from Columbia, MD)..

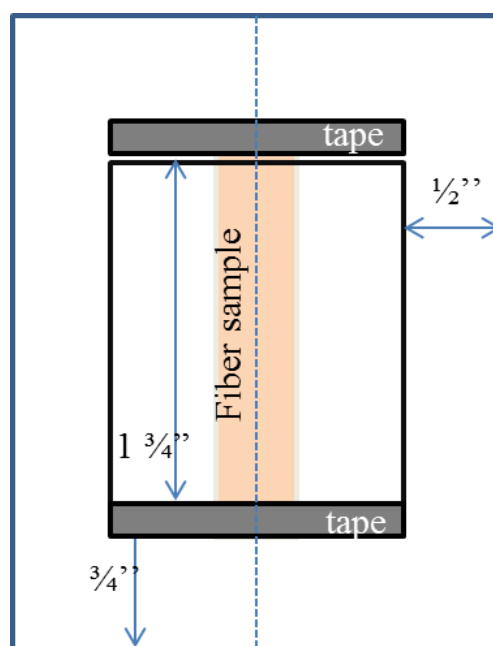*Figure 10.* Fiber sample holder.

Trapezium Lite software was used to input data collection parameters and were set to displacement rate $V_1= 10mm/ min$ and data acquisition time= 500 ms for the10 N load cell. Additional software parameters were selected to collect the output time (seconds), force (Newton's), and stroke (millimeters) data. To test, the sample holder was centered and tightened

between the bottom and top clamps. Both sides of the sample holder were cut to release tension before measurements were collected. In the software, the force and stroke were zeroed to calibrate the system and the test was started. After each test was completed, the exported raw data was saved in a spreadsheet and used to extrapolate the strain and stress from the force and displacement data collected. Stress was calculated by dividing the force by the cross sectional area and the strain was calculated by dividing the elongation length by the original length of the fiber sample. Stress-strain curves were created for each trial to evaluate the Young's Modulus and Ultimate Tensile Strength of the fiber samples.

   3.4.5 Wettability analysis. For wetting analysis fiber samples were cut in small rectangles from the original source of each ratio. Dynamic Contact Angle Tester used SCA 20 software to measure the contact angles that acknowledged which fiber ratios were hydrophilic or hydrophobic. Figure 11 shows the quantitative measure of contact angle which measures the hydrophobicity and hydrophilicity of solid fiber membrane.
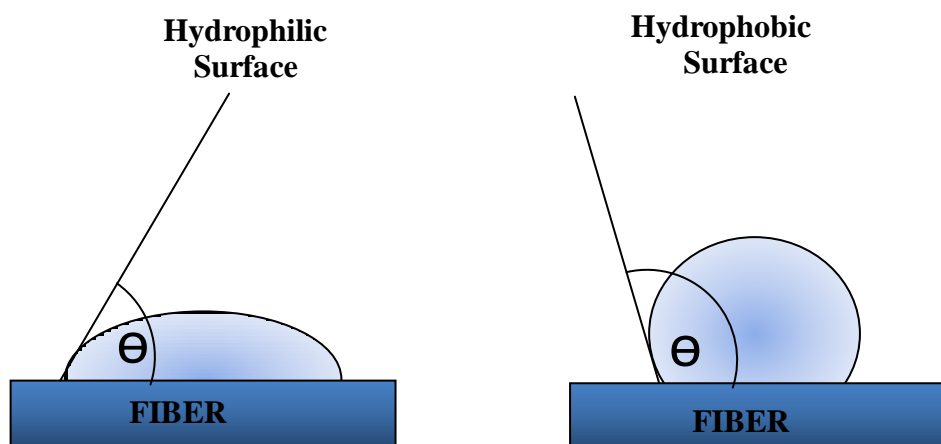

Figure 11. Wettability analysis set up.

3.5 In vitro Study

3.5.1 Degradation. Fiber samples one week and 7 week degradations were prepared and experimented from three samples of each ratio from PCL/Keratin 100/0, 90/10, 80/20, 70/30. Samples were cut into rectangular profiles and were placed in individual labeled conical tubes. The fiber samples were immersed in Phosphate Buffer Saline (PBS) solution for one and seven week period at 37ºC. After the allotted time periods, fibers were rinsed, pat dry and placed on the freeze dryer to be analyzed under SEM.

3.5.2 Cytotoxicity analysis. Four different 24 well plates are separated into the following PCL/ Keratin ratios: A= 100/0, B=90/10, C=80/20, and D=70/30. To clean fibers, 80% ethanol was used. Each sample was submerged for 5 minutes in the 24 well plates. A fresh 80% ethanol (5 ml) was poured into the wells for a repeat soaking process. Then each fiber was rinsed and submerged with PBS for 5 minutes and repeated as well. Lastly, all fibers were rinsed with DI water for 5 mins and repeated to complete the cleaning process. Fibers were placed in 15 ml sized conical tubes and put on the freeze dryer for 1 hour to dry. When complete dryness was achieved, the clean fibers were stored back in the 24 well dried plates. Fibers were then sealed with Kwik-Sil on 14mm glass slides. A schematic in Figure 12 shows how fiber was placed on top of the glass. All fibers were cut into 14mm x 14mm sized squares to provide full coverage over the glass slides. Appendix A shows PCL/Keratin ratio sample preparation as an example.
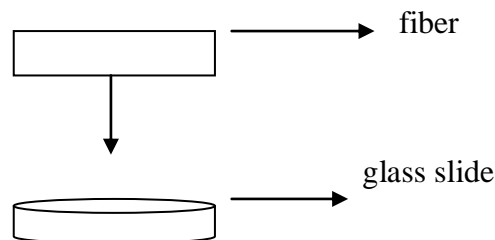

Figure 12. Schematic of fiber cell testing.

For cytotoxicity analysis the 24 well plates prepared in the above procedure were used. Sterilization of each sample with sterile DI water was carried out by submerging with 70% EtOH for 20 minutes and washed. Fibroblast 3T3 cells with passage 20 were plated 62,000 cell/cm^2 in 24 wells with 1 ml of media (10FCS/DMEN + L-glutamine and antibiotics). Cells were grown in 37^{0}C incubator for 24 hours (5% CO_2). Alamar Blue Assay, a non-toxic scalable method was used to assess whether cells have enough energy to proliferate. Resazurin was added to 3 wells/ condition: 200µl resazurin + 800µl media resulting with a final volume of 2ml. After 1 hour, 4 x 100µl/sample was removed to wells of 96-well plate for reading on a microplate reader at 530nm EX/ 590nm EM. The last column of wells got Cell Tracker Red in media, not resazurin. These were imaged on a florescent microscope. Lastly all wells were fixed with 4% paraformaldehyde/ 2% glut for 20 minutes. Wells were washed 3x with PBS and stored at 4 ℃ until it dehydrated in alcohols to 100% EtOH and put in a desiccator for 30 mins then was wrapped in parafilm.

CHAPTER 4

Results

4.1 Extraction of Keratin

    4.1.1 Yields. The amount of hair used initially was compared to the amount of powdered keratin that was actually extracted after lyophilization. The yield was approximately 2.5%. The extraction process was extensive with numerous multi steps. Several batches of keratin powder were prepared to obtain sufficient amount of keratin powder needed to create solutions for electrospinning. The fact that the yield remained low, encouraged frequent extractions to occur simultaneously.

    4.1.2 Consistency of extracted keratin. The consistency of the extracted keratin depended on the consistency of the methods and skills performed throughout the process. Many adjustments were established for each step to ensure consistency between trials. Close documentation of timing was considered as well.

4.2 Electrospinning Preparation and Considerations of Spinning Techniques

    The polymer solutions were mixed for a range of 30 minutes to 2 hours depending on the ratio. The PCL/keratin ratio of 60/40 took the longest to mix homogeneously in the glass container by vortex. The PCL/ Keratin with ratio of 70/30 were mixed for over a one hour period as well. The viscosities of the two dissolved solutions changed in how it blended from the difference in ratios. Thus, prepared solution was charged with high voltage. The ground collector remained stationary and fibers from each ratio were able to deposit in one section at a time, and the collector was hand rotated to collect remaining fibers throughout the electrospinning process. The images in Figure 13 represent a visual of the formation of the 100/0, 90/10, 80/20, and 70/30 PCL/Keratin fibers. Collection of fibers from different ratios ranged from 30 mins to 1.5 hours.
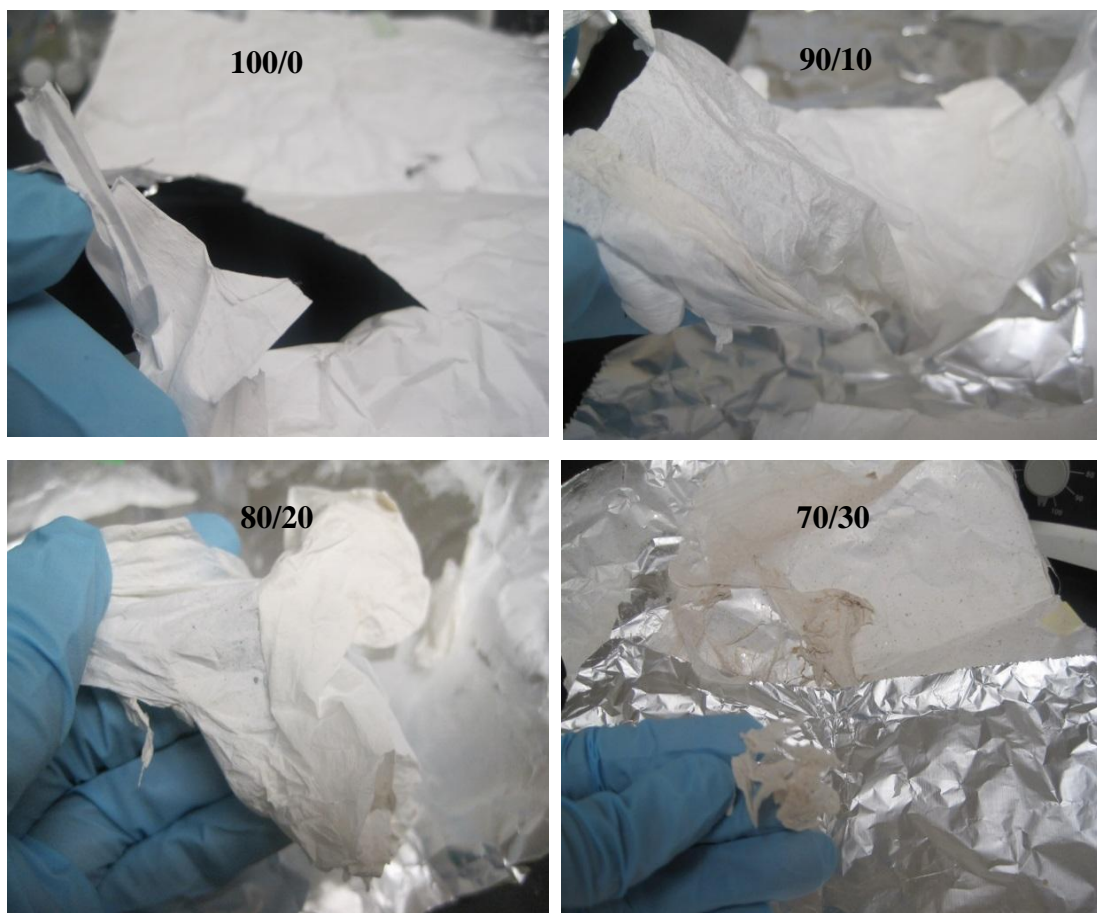
Figure 13. Electrospun nonwoven mesh of PCL/Keratin ratios.

4.3 Nanofiber Characterization

4.3.1 Scanning electron microscopy. The image in Figure 14 is of 100% PCL electrospun fiber at 500 magnifications and 10k magnification. It was necessary to create the 100% PCL fiber to optimize the electrospinning set up and to form successful bead free samples. An entire uniform sample of 100% PCL was collected on aluminum foil and was easily removable by gently pealing the fiber from the attached surface. The thickness of the fiber provided sturdiness to the nonwoven mesh structure. The remaining SEM morphology of PCL/Keratin ratios of are imaged in the degradation results, and labeled as the control.

Figure 14. SEM image of PCL nanofiber.
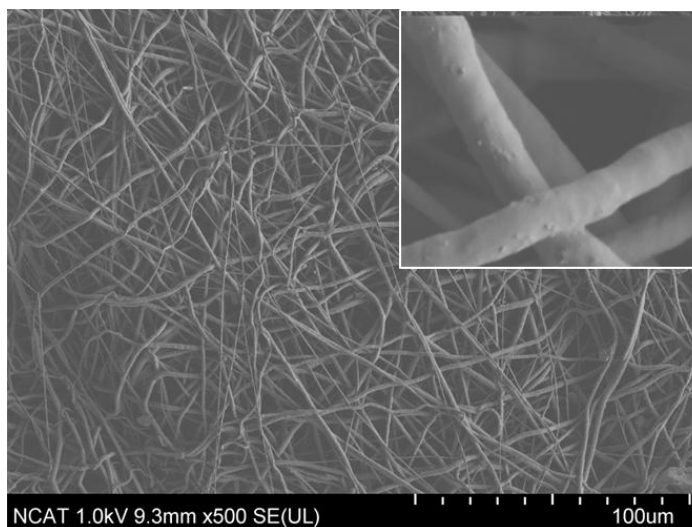
4.3.2 Fourier transform infrared spectroscopy. Spectra of PCL/Keratin nanofibers

were measured in Figure 15 and represent the bonding between PCL compounds and keratin.

The major peak for all the fiber samples is measured at 1722 cm^{-1} which agrees with the standard

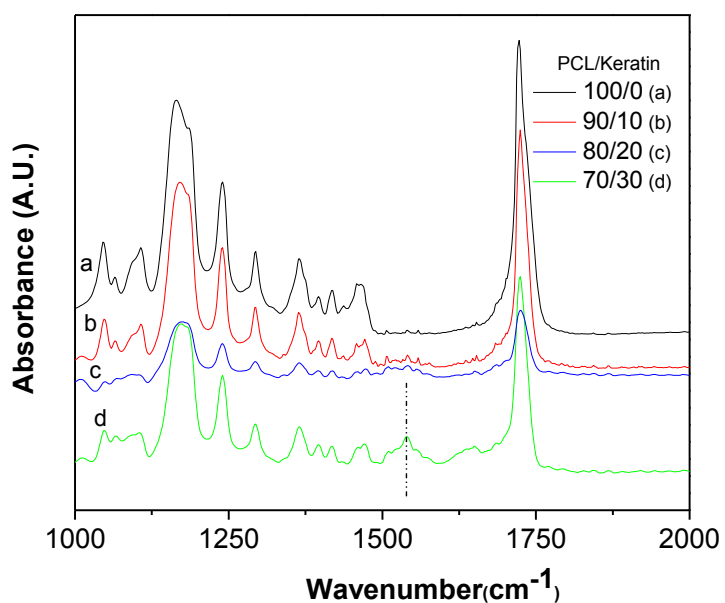basic measurement of PCL absorption band.

Figure 15. FTIR PCL/Keratin nanofibers with different ratios.

The major PCL peak corresponds to the carbonyl groups. When keratin is added in the remaining ratios 90/10, 80/20 and 70/30, it interferes with the functional groups PCL. The stretching of ester bonds are represented within the 1750-1735 cm^{-1} range. A highlighted characteristic peak of keratin was observed around 1540 cm^{-1} shown in the dotted line indicated for PCL/Keratin 70/30 fiber ratio.

4.3.3 X-ray diffraction. The peaks in Figure 16 below represented the crystalline structure of the PCL /Keratin structure within the fibers. PCL/Keratin fiber ratios of 90/10, 80/20, 70/30, and 50/50 were measured.. The characteristic diffraction peaks of PCL are 21.310 ^{0} and 23.66 ^{o}.
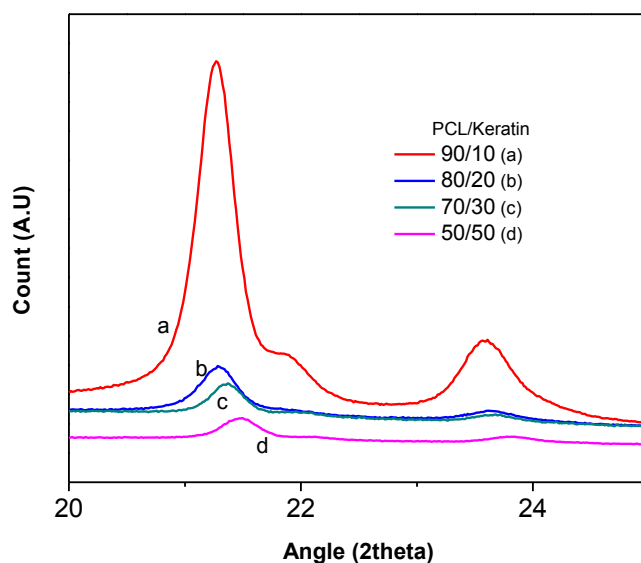

Figure 16. XRD PCL/Keratin fiber results.

The characteristic peaks shown in Table *5* are very close in value to PCL alone. The major peak for the PCL/Keratin ratios range from 21.25 ^{0} to 21.48 ^{0} and the secondary peak range from 23.55^{0} to 23.79^{0}. The shift in degree indicates a decrease in crystallinity of PCL with the addition of keratin.

Table 5

XRD major peaks

Ratio	1st Peak	2nd Peak
90/10	21.25°	23.55°
80/20	21.29°	23.60°
70/30	21.38°	23.59°
60/40	21.48°	23.79°

4.3.4 Mechanical strength tensile test. PCL/Keratin mechanical tests were performed for the following ratios: 100/0, 90/10, and 80/20. Figure 17 shows the resulting plot of stress verses strain curves. The first indication of deformation within the materials is seen in the first bend each curve.
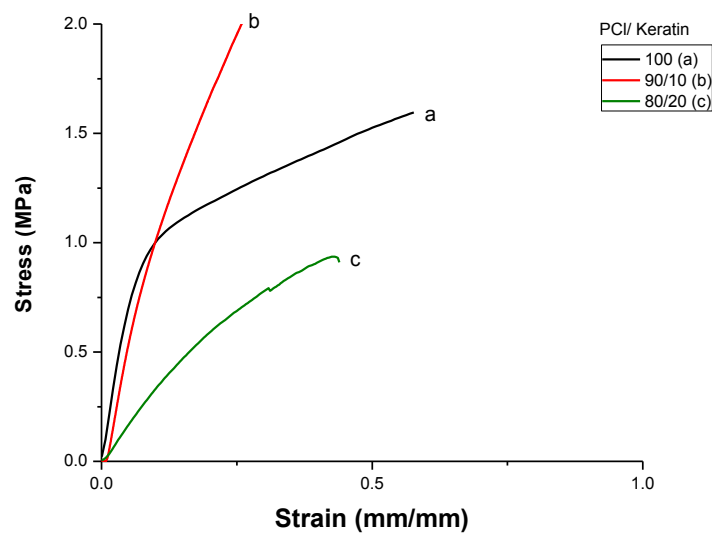

Figure 17. Mechanical testing on PCL/Keratin ratios.

Figure 18 is the result of ultimate tensile strength and Young's modulus obtained from stress-strain curves. The ultimate tensile strength represents the highest quantity of stress that each PCL/Keratin fiber sample can withstand while it was elongated with the force applied, and actually breaks.
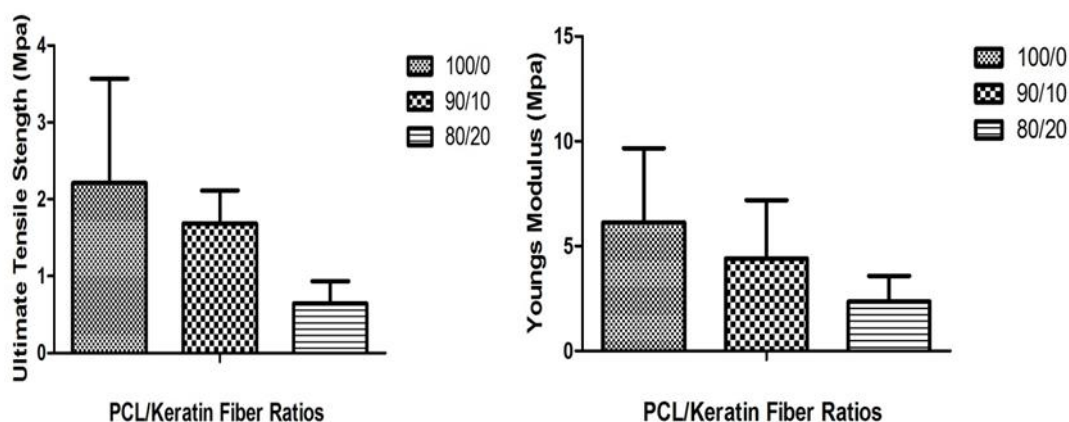
*Figure 18.*Ultimate tensile strength and Young's modulus plotted data.

4.3.5 Wettability Analysis. The results shown in Table *6* were the given angles of wetting analysis of PCL/ Keratin fibers with ratios of 100/0, 90/10, and 80/20. The contact angle was determined is listed below. From these results the change in hydrophobic and hydrophilic properties from the addition of keratin to each PCL/Keratin fiber sample were evaluated.

Table 6

Wettability Analysis

Ratios	Contact Angle
100/0	81.3°
90/10	78.7°
80/20	69.2°
70/30	62.9°

4.4 In Vitro Study

  4.4.1 Degradation. All the degradation nanofibers were imaged under SEM. Figure 19 shows the top panel of PCL/Keratin nanofibers as a control, and the bottom two panels display the SEM images of nanofibers after 1 and 7 weeks.
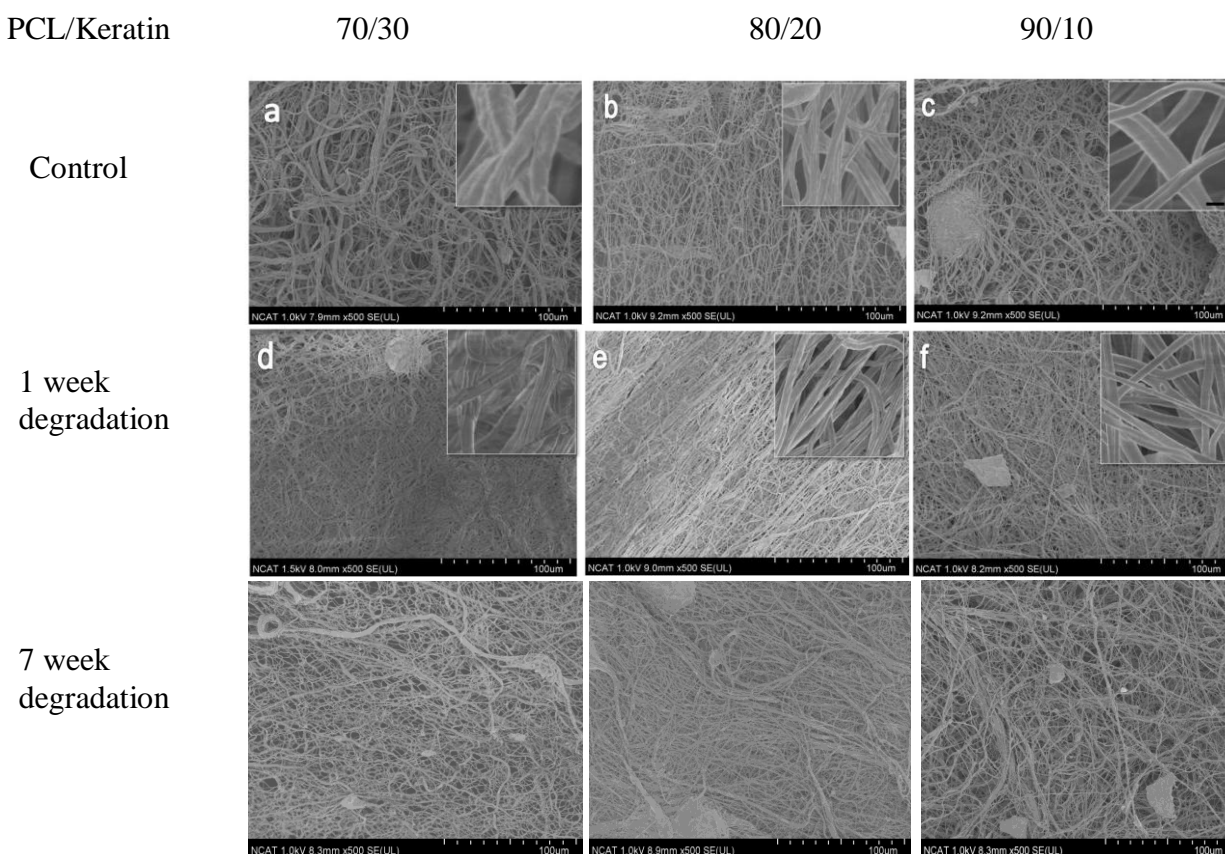
Figure 19. SEM images of 1 and 7 week degradation vs control PCL/Keratin fibers.

  4.4.2 Cytotoxicity. Fibroblast 3T3 cells are imaged under SEM at 500 and 2,000 magnification in contact with PCL/Keratin 90/10 ratio fibers (Figure 20). The darker areas on both images indicate the location of each fibroblast cells attached on top of and throughout the nanofiber topography. Cellular biocompatibility was successfully achieved.
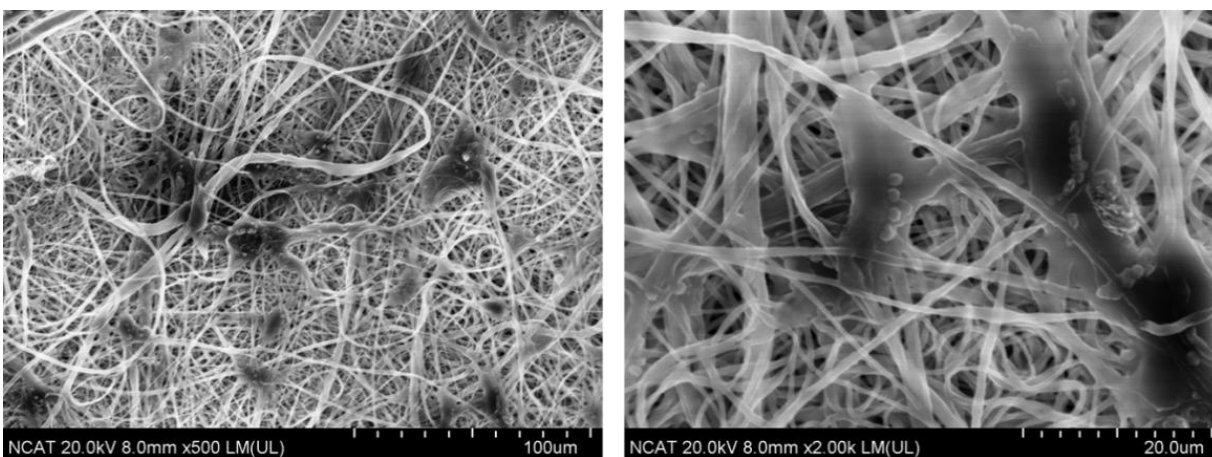
Figure 20. Morphology of 3T3 fibroblast cells seeded on PCL/Keratin nanofiber membrane.

In the following graph of percent verses PCL/Keratin fibers, determined that no samples were statistically different from the control glass cover slide. The results provide confirmation that PCL/Keratin nanofibers do not induce harmful or toxic effects on fibroblast 3T3 cells. PCL/Keratin ratios are labeled Con= control, A= 100/0, B=90/10, C= 80/20, and D=70/30.
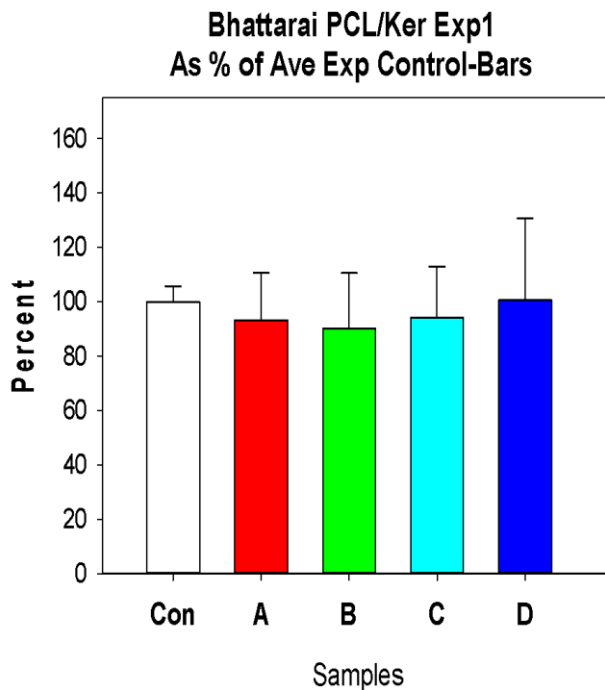
Figure 21. Cytotoxicity results of PCL/Keratin fibers and 3T3 cells.

CHAPTER 5

Discussion and Future Research

During extraction, hair was moderately oxidized with an oxidizing agent of peracetic acid which kept some bonds intact and partially cleaved some disulfide bonds. The consistency of the extracted keratin depended on the consistency of the techniques performed throughout the extraction process. After several trial experiments the extraction techniques were mastered and documented carefully in order to continue a steady outcome of keratin products necessary to create successful polymer blends with PCL for electrospinning fibers. The yields however of the keratin extracts in powder form were very low. Modifications were altered from preparations for keratin biomaterials techniques (Sierpinski et al., 2008) , can be further modified to extract a higher yield. The morphology of keratin powder produced after lyophilization changed throughout many trials. Some keratin powder only was located at the bottom of the glass jar in uniform position. Other freeze dried powders attached to the sides of the glass. These observations were handled accordingly from the differences in trials to successfully create the solution.

Preparation of the polymer solutions which included dissolving PCL in Trifluoroethanol (TFE) at the chosen concentration and keratin in water at the chosen concentration were both recommended computations from previous studies. In many previous studies water soluble and insoluble proportions proved successful in mixing. When PCL was chosen specifically as the synthetic polymer to blend with natural polymers, a well defined procedure is needed. Regarding the fact that PCL is able to dissolve in TFE at a reliable rate, results were successful within a 12 hour period. Keratin easily dissolved in DI water with the range of a few minutes to up to an hour in time. The blending technique developed for PCL and keratin in this research, was similar

to the previously developed technique for electrospinning of keratin and polyethylene oxide (PEO) blend solution (Aluigi et al., 2007).

When electrospinning process was executed, the variation of fiber formation was not only dependent due to the concentration of the polymer solutions, but also was a resultant of optimized parameters within the electrospinning set up. As expected from previous experimentation and the properties PCL, successful electrospun PCL fibers were consistently formed. The thickness of the PCL fiber exceeded the PCL/Keratin fiber thickness of 90/10, 80/20, and 70/30. PCL remains to uphold as a common biomaterial used in peripheral nerve guides mainly for the mechanical strength potential. The PCL fibers encompassed the entire aluminum foil sheet on the grounded collector superior to any other fiber ratio. The contents were overall flat and plentiful for easy removal from the aluminum foil. For the variety of physical and chemical testing that was performed, the PCL fibers were manageable and available to cut in precise measurements.

The presence of keratin in the PCL/Keratin nanofibers was confirmed using FTIR. The results show a differentiation of characterization peaks from the original 100 % PCL peak to the addition of keratin. In previous study, stretching of the ester band of PCL at $1724cm^{-1}$ was observed as a major peak on PCL nanofibers (Prabhakaran, Venugopal, Chan, & Ramakrishna, 2008). As shown in the PCL/Keratin 70/30 ratio, a characteristic peak around $1540 \ cm^{-1}$ indicated presence of keratin. The rate of degradation and the capability of nanofibers retaining reliability over a period of time can be determined, as suggested in a similar PCL based nanofibers study by FTIR (Bhattarai, 2009).

From XRD results of the PCL/Keratin fiber, the shift of ratio compositions explains how the addition of the keratin protein effects the composition of PCL. From previous

experimentation of PCL data of XRD, the diffraction peaks were shown at 21.5 º and 23.6º

(Johnson et al., 2005). Therefore, the measured XRD values for ratios 90/10, 80/20, 70/30, and

50/50 PCL/Keratin fell very closely with that standard angle for these two main peaks in PCL's

structure. As keratin is added to the peaks, causes a slight shift with significant decrease in

intensity of peaks which indicates disruption of PCL crystalline structure and encourages

miscibility and change in morphology.

Blended fibers give an advantage of combining natural and synthetic polymer properties

that are necessary to design conduits with desired properties for peripheral nerve guides.

Important features that are considered are the ultimate tensile strength and the Young's modulus

of the nanofibers. Ultimate tensile data collected from PCL/Keratin fibers compared much less

than peripheral nerve *in situ* has a tensile strength of approximately 11.7 MPa (Rydevik et al.,

1990; Weir, Buchanan, Orr, Farrar, & Boyd, 2004). Knowing the desired tensile strength helps to

identify the best suited biodegradable fiber to use to create conduits from nerve regeneration

purposes. The decrease of value for Young's modulus and ultimate tensile strength account to

the addition of keratin present within the different ratios.

The degradation study as carried by observing SEM images showed that in a 1 week

period, fibers did not change the morphology compared to week 7 time period. The images were

captured in three resolutions and observed at low magnification, the degraded PCL/Keratin 80/20

ratio appeared to merge together across the fiber image after 7 weeks compared to the control.

The PCL/ Keratin 70/30 ratio degraded the fastest over the 7 week period, which changed the

morphology the greatest from all other ratios. PCL/Keratin fiber ratios contained more keratin

became more hydrophilic, as confirmed in the wetting analysis data collected. The contact angle

decreased as expected and seen in similar studies of measuring blended natural and synthetic

polymer ratios. Due to this modification, the rate of degradation of PCL was increased as expected.

Cytotoxicity testing was only performed over a 24 hour period and determined that PCL/keratin fibers are not toxic for 3T3 fibroblast cells. Alamar Blue results showed no samples were significantly different from the control glass slide, by comparing the percent of toxic effect expressed. To achieve more conclusive results, more PCL/Keratin fiber samples are needed to test up to a 1 week time period. Additional trials will be performed to produce adequate results. SEM morphology of cells imaged on PCL/Keratin fibers showed how the 3T3fibroblast cells were able to penetrate throughout the fibers and make good contact. Excellent morphology of nanofiber/cell was observed in the PCL/ Keratin (90/10) compared to other ratios.

Damaged peripheral nerves require for the distal and proximal nerve ends to reunite and grow back successfully in order to restore function. A major component depends on size of the nerve gap. Currently available nerve guidance conduits have been limited to gap sizes ≤ 3cm. Historically, the golden standard for smaller gap sizes are using autographs, suturing, or allowing natural regeneration to take place. Yet autographs may not ensure the desired healthy function after regeneration is complete. Therefore, the need for a improved solution is being investigated through using biomaterials such as PCL and keratin to improve peripheral nerve gap damage.

Future direction in this research will include generating additional weight percent blended polymer nanofibers through the use of electrospinning technology. Exploring the potential of filling conduits with hydrogels to enhance cellular regeneration properties will be investigated in future experimentation. Schwann and PC12 cell cytotoxicity testing will also be conducted in the continued work, to study and compare proliferation and migration affects of the neuronal cells on the PCL/Keratin fibers. Each nanofibers ratio combination will be rolled into

conduits and cellular adherence, degradation, mechanical strength, and proliferation will be tested and observed as well. These factors are detrimental to the stability and pliability of the nanofibers to be created into nerve guidance conduits. Ultimately, *in vivo* studies of PCL/Keratin conduits will be created as pictured in Appendix B. As hypothesized and objected for this research, PCL/Keratin based nanofibers have the potential and desired properties of mechanical strength and cellular compatibility that will provide enhancement of damaged peripheral nerve gap sites and will opportunely degrade in the process of healing.

References

Alonso, L., & Fuchs, E. (2006). The hair cycle. *J Cell Sci, 119*(3), 391-393. doi: Doi 10.1242/Jcs02793

Aluigi, A., Varesano, A., Montarsolo, A., Vineis, C., Ferrero, F., Mazzuchetti, G., & Tonin, C. (2007). Electrospinning of keratin/poly(ethylene oxide) blend nanofibers. *Journal of Applied Polymer Science, 104*(2), 863-870.

Battiston, B., Tos, P., Geuna, S., Giacobini-Robecchi, M. G., & Guglielmone, R. (2000). Nerve repair by means of vein filled with muscle grafts. II. Morphological analysis of regeneration. *Microsurgery, 20*(1), 37-41.

Beachley, V., & Wen, X. (2010). Polymer nanofibrous structures: Fabrication, biofunctionalization, and cell interactions. *Prog Polym Sci, 35*(7), 868-892.

Bhattarai, N., Li, Z., Gunn, J., Leung, M., Cooper, A., Edmondson, D., Zhang, M. (2009). Natural-Synthetic Polyblend Nanofibers for Biomedical Applications. *Advanced Materials, 21*(27), 2792-2797.

BN., C. (2011). Peripheral Nerve Injuries.

Cao, H., Liu, T., & Chew, S. Y. (2009). The application of nanofibrous scaffolds in neural tissue engineering. *Advanced Drug Delivery Reviews, 61*(12), 1055-1064.

Carothers, W. H. (1929). STUDIES ON POLYMERIZATION AND RING FORMATION. I. AN INTRODUCTION TO THE GENERAL THEORY OF CONDENSATION POLYMERS. *Journal of the American Chemical Society, 51*(8), 2548-2559.

Cha, Y., & Pitt, C. G. (1990). The biodegradability of polyester blends. *Biomaterials, 11*(2), 108-112.

Clark, R. A. F. (1985). Cutaneous tissue repair: Basic biologic considerations. I. *J Am Acad Dermatol, 13*(5, Part 1), 701-725.

Cooper, A., Bhattarai, N., & Zhang, M. Q. (2011). Fabrication and cellular compatibility of aligned chitosan-PCL fibers for nerve tissue regeneration. *Carbohydrate Polymers, 85*(1), 149-156.

Coulombe, P. A., & Omary, M. B. (2002). 'Hard' and 'soft' principles defining the structure, function and regulation of keratin intermediate filaments. *Current Opinion in Cell Biology, 14*(1), 110-122.

Daly, W., Yao, L., Zeugolis, D., Windebank, A., & Pandit, A. (2012). A biomaterials approach to peripheral nerve regeneration: bridging the peripheral nerve gap and enhancing functional recovery. *Journal of The Royal Society Interface, 9*(67), 202-221.

E, G. (1989). Morphometry of unmyelinated nerve fibers. *Clinical Neuropathology 8*, 179-187.

Evans, G. R. D. (2001). Peripheral nerve injury: A review and approach to tissue engineered constructs. *The Anatomical Record, 263*(4), 396-404.

Filler, A. M. (2004). Nerve Structure. *Do You Really Need Back Surgery: A Surgeon's Guide to Neck and Back Pain and How to Choose Your Treatment*, 288.

Ghasemi-Mobarakeh, L., Prabhakaran, M. P., Morshed, M., Nasr-Esfahani, M. H., & Ramakrishna, S. (2008). Electrospun poly(epsilon-caprolactone)/gelatin nanofibrous scaffolds for nerve tissue engineering. [Research Support, Non-U.S. Gov't]. *Biomaterials, 29*(34), 4532-4539. doi: 10.1016/j.biomaterials.2008.08.007

Göpferich, A. (1996). Mechanisms of polymer degradation and erosion. *Biomaterials, 17*(2), 103-114.

Hill, P., Brantley, H., & Van Dyke, M. (2010). Some properties of keratin biomaterials: Kerateines. *Biomaterials, 31*(4), 585-593.

Huggins, M. L. (1943). The Structure of Fibrous Proteins. *Chemical Reviews, 32*(2), 195-218.

Huggins, M. L. (1980). Structure of β-Keratin. *Macromolecules, 13*(3), 465-470. doi: 10.1021/ma60075a002

Itoh, S., Yamaguchi, I., Suzuki, M., Ichinose, S., Takakuda, K., Kobayashi, H., . . . Tanaka, J. (2003). Hydroxyapatite-coated tendon chitosan tubes with adsorbed laminin peptides facilitate nerve regeneration in vivo. *Brain Research, 993*(1), 111-123.

Jiang, X., Lim, S. H., Mao, H.-Q., & Chew, S. Y. (2010). Current applications and future perspectives of artificial nerve conduits. *Experimental Neurology, 223*(1), 86-101.

Johnson, E. O., Zoubos, A. B., & Soucacos, P. N. (2005). Regeneration and repair of peripheral nerves. *Injury, 36*(4, Supplement), S24-S29.

Katoh, K., Tanabe, T., & Yamauchi, K. (2004). Novel approach to fabricate keratin sponge scaffolds with controlled pore size and porosity. *Biomaterials, 25*(18), 4255-4262.

Kelleher, M., Al-Abri, R., Eleuterio, M., Myles, L., Lenihan, D., & Glasby, M. (2001). The use of conventional and invaginated autologous vein grafts for nerve repair by means of entubulation. *British Journal of Plastic Surgery, 54*(1), 53-57.

Koh, H., Yong, T., Teo, W., Chan, C., Puhaindran, M., Tan, T., . . . Ramakrishna, S. (2010). In vivo study of novel nanofibrous intra-luminal guidance channels to promote nerve regeneration. *Journal of neural engineering, 7*(4), 046003.

Kokai, L. E., Bourbeau, D., Weber, D., McAtee, J., & Marra, K. G. (2011). Sustained growth factor delivery promotes axonal regeneration in long gap peripheral nerve repair. [Research Support, N.I.H., Extramural

Research Support, U.S. Gov't, Non-P.H.S.]. *Tissue Engineering Part A, 17*(9-10), 1263-1275.

    doi: 10.1089/ten.TEA.2010.0507

Lam, C. X., Savalani, M. M., Teoh, S.-H., & Hutmacher, D. W. (2008). Dynamics of in vitro

    polymer degradation of polycaprolactone-based scaffolds: accelerated versus simulated

    physiological conditions. *Biomedical Materials, 3*(3), 034108.

Li, D., & Xia, Y. N. (2004). Electrospinning of nanofibers: Reinventing the wheel? *Advanced*

    Materials, 16(14), 1151-1170.

Lin, Y. C., Ramadan, M., Van Dyke, M., Kokai, L. E., Philips, B. J., Rubin, J. P., & Marra, K. G.

    (2012). Keratin gel filler for peripheral nerve repair in a rodent sciatic nerve injury

    model. [Research Support, U.S. Gov't, Non-P.H.S.]. *Plastic Reconstruction Surgery*

    129(1), 67-78.

Lyons, K. M., Pelton, R., & Hogan, B. (1990). Organogenesis and pattern formation in the

    mouse: RNA distribution patterns suggest a role for bone morphogenetic protein-2A

    (BMP-2A). *Development, 109*(4), 833-844.

Mackinnon, S. (1989). Surgical management of the peripheral nerve gap. *Clinics in plastic*

    surgery, 16(3), 587.

Matsuyama, T., Mackay, M., & Midha, R. (2000). Peripheral Nerve Repair and Grafting

    Techniques: A Review. *Neurologia medico-chirurgica, 40*(4), 187-199.

Moll, R., Divo, M., & Langbein, L. (2008). The human keratins: biology and pathology.

    [Article]. *Histochemistry & Cell Biology, 129*(6), 705-733.

Mukhatyar, V., Karumbaiah, L., Yeh, J., & Bellamkonda, R. (2009). Tissue engineering

    strategies designed to realize the endogenous regenerative potential of peripheral nerves.

    Advanced Materials, 21(46), 4670-4679.

Nectow, A. R., Marra, K. G., & Kaplan, D. L. (2012). Biomaterials for the development of

peripheral nerve guidance conduits. [Research Support, N.I.H., Extramural

Research Support, Non-U.S. Gov't]. *Tissue Engineering Part B Reviews, 18*(1), 40-50. doi:

10.1089/ten.TEB.2011.0240

Paulina S. Hill, P. D., 1 Peter J. Apel, M.D., Ph.D.,2 Jonathan Barnwell, M.D.,2 Tom Smith,

Ph.D.,2, & L. Andrew Koman, M. D., 2 Anthony Atala, M.D.,1 and Mark Van Dyke,

Ph.D. (2011). Repair of Peripheral Nerve Defects in Rabbits

Using Keratin Hydrogel Scaffolds. *TISSUE ENGINEERING: Part A, Volume 17*, 1499-1505.

Popescu, C., & Hocker, H. (2007). Hair-the most sophisticated biological composite material.

Chemical Society Reviews, 36(8), 1282-1291.

Prabhakaran, M. P., Venugopal, J., Chan, C. K., & Ramakrishna, S. (2008). Surface modified

electrospun nanofibrous scaffolds for nerve tissue engineering. *Nanotechnology, 19*(45),

455102.

Prabhakaran, M. P., Venugopal, J. R., Chyan, T. T., Hai, L. B., Chan, C. K., Lim, A. Y., &

Ramakrishna, S. (2008). Electrospun biocomposite nanofibrous scaffolds for neural tissue

engineering. [Research Support, Non-U.S. Gov't]. *Tissue Engineering Part A, 14*(11),

1787-1797. doi: 10.1089/ten.tea.2007.0393

Reichl, S. (2009). Films based on human hair keratin as substrates for cell culture and tissue

engineering. *Biomaterials, 30*(36), 6854-6866.

Reneker, D. H., & Chun, I. (1996). Nanometre diameter fibres of polymer, produced by

electrospinning. *Nanotechnology, 7*(3), 216-223.

Reneker, D. H., Yarin, A. L., Fong, H., & Koombhongse, S. (2000). Bending instability of electrically charged liquid jets of polymer solutions in electrospinning. *Journal of Applied Physics, 87*(9), 4531-4547.

Rutkowski, G. E., Miller, C. A., Jeftinija, S., & Mallapragada, S. K. (2004). Synergistic effects of micropatterned biodegradable conduits and Schwann cells on sciatic nerve regeneration. *Journal of neural engineering, 1*(3), 151.

Rydevik, B. L., Kwan, M. K., Myers, R. R., Brown, R. A., Triggs, K. J., Woo, S. L. Y., & Garfin, S. R. (1990). An in vitro mechanical and histological study of acute stretching on rabbit tibial nerve. *Journal of Orthopaedic Research, 8*(5), 694-701.

Sierpinski, P., Garrett, J., Ma, J., Apel, P., Klorig, D., Smith, T., . . . Van Dyke, M. (2008). The use of keratin biomaterials derived from human hair for the promotion of rapid regeneration of peripheral nerves. [Research Support, Non-U.S. Gov't]. *Biomaterials, 29*(1), 118-128.

Stoll, G., Griffin, J., Li, C., & Trapp, B. (1989). Wallerian degeneration in the peripheral nervous system: participation of both Schwann cells and macrophages in myelin degradation. *Journal of neurocytology, 18*(5), 671-683.

Sunderland, S. (1951). A classification of peripheral nerve injuries producing loss of function. *Brain, 74*(4), 491-516.

Tachibana, A., Furuta, Y., Takeshima, H., Tanabe, T., & Yamauchi, K. (2002). Fabrication of wool keratin sponge scaffolds for long-term cell cultivation. *Journal of Biotechnology, 93*(2), 165-170.

Tupper, J. W. (1991). Fascicular repair. *Operative Nerve Repair and Reconstruction, 1*, 295-303.

Varesano, A., Aluigi, A., Vineis, C., & Tonin, C. (2008). Study on the shear viscosity behavior of keratin/PEO blends for nanofibre electrospinning. *Journal of Polymer Science Part B: Polymer Physics, 46*(12), 1193-1201.

Waddell, R. L., Marra, K. G., Collins, K. L., Leung, J. T., & Doctor, J. S. (2003). Using PC12 cells to evaluate poly(caprolactone) and collagenous microcarriers for applications in nerve guide fabrication. [Evaluation Studies

Research Support, Non-U.S. Gov't]. *Biotechnology Progress, 19*(6), 1767-1774.

Weir, N. A., Buchanan, F. J., Orr, J. F., Farrar, D. F., & Boyd, A. (2004). Processing, annealing and sterilisation of poly-l-lactide. *Biomaterials, 25*(18), 3939-3949.

Woodruff, M. A., & Hutmacher, D. W. (2010). The return of a forgotten polymer— Polycaprolactone in the 21st century. *Progress in Polymer Science, 35*(10), 1217-1256.
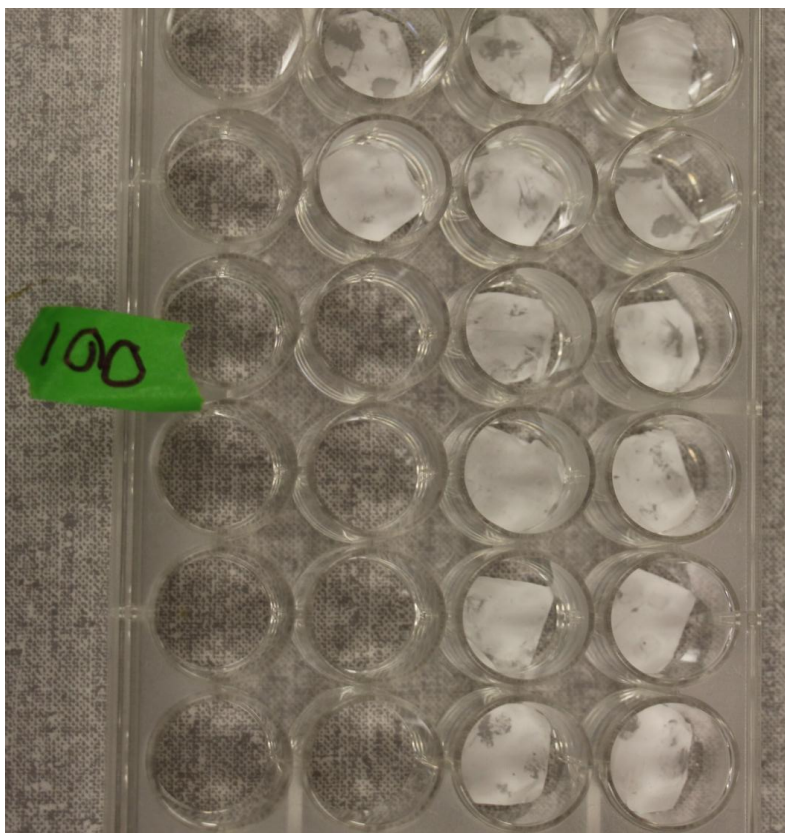
Appendix A

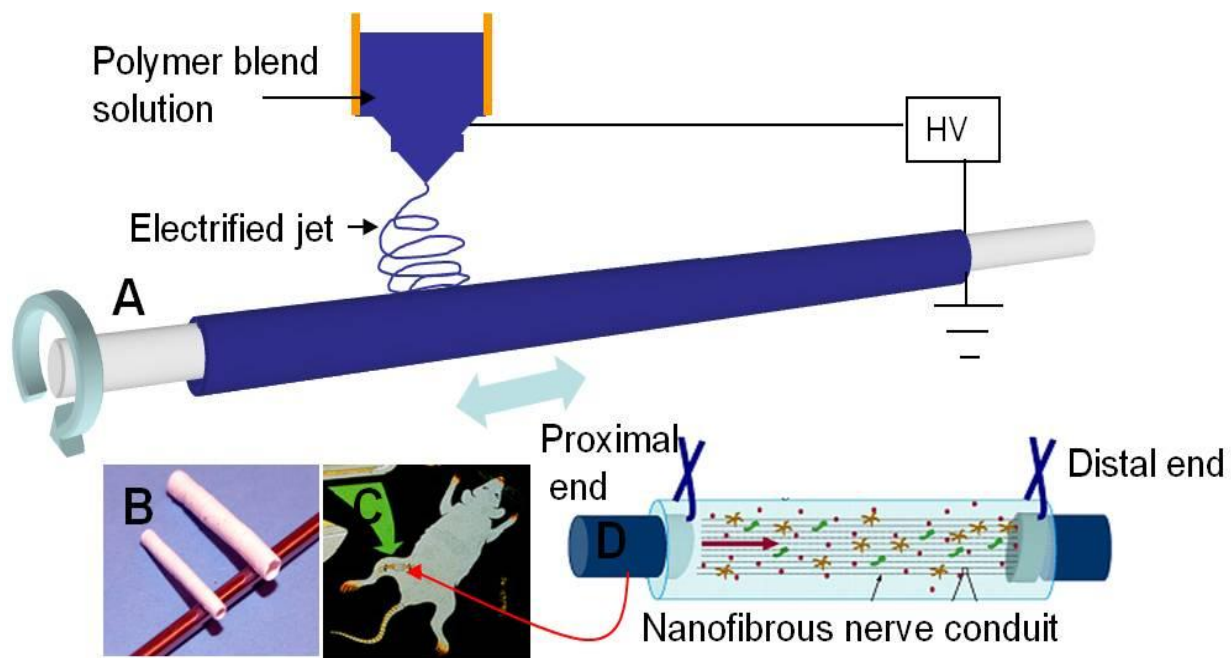Figure. Cytotoxicity testing prepared samples.

Appendix B

Figure. Future work for creating PCL/Keratin based conduits for in vivo study.